Journal of Hazardous Materials, 34 (1993) 123–150
Elsevier Science Publishers B.V., Amsterdam

Unconfined deflagrative explosion without turbulence: Experiment and model

J.C. Leyer[a,*], D. Desbordes[a], J.P. Saint-Cloud[a] and A. Lannoy[b]

[a] *Laboratoire d'Energétique et de Détonique (URA 193 CNRS) ENSMA — Université de Poitiers, Rue Guillaume VII, 86034 Poitiers (France)*
[b] *EDF — Direction des Etudes et Recherches, 25, Allée Privée, Carrefour Pleyel, 93206 Saint-Denis Cedex 1 (France)*

(Received March 3, 1992; accepted August 10, 1992)

Abstract

This paper reviews laboratory, balloon and open-field experiments, which have been performed to study the deflagration regime in free air. In the first part, the paper considers briefly the different models available to estimate deflagrative unconfined explosion effects, without turbulence. Then a description is given of the known tests conducted, which indicates the effective scale of the various experiments, their operating conditions and the kind of the measurements done. The main results are presented and discussed in some detail to assess the role on the explosion yields of important parameters such as the fuel concentration gradients, the shape and size of the inflammable mixture, and the ignition energy. The overall conclusion of this survey is that inflammable mixtures drifting over open field and ignited, will burn with a low flame speed and consequently will generate very weak pressure effects.

1. Introduction

In the design and construction of industrial installations, it is necessary, for safety purposes, to take into account the potential explosion hazards resulting from accidental spills. These take the form of a massive release of a dangerous product, generally a hydrocarbon, followed by the formation in the atmosphere of an inflammable cloud. Depending on the weather conditions and topography, such a cloud may drift, and if it is ignited, the pressure wave created by the explosion may cause serious damage, even at considerable distances. In order to protect the safety functions of a plant, where large quantities of inflammable materials are processed, stored or transported, it appears necessary to assess the overloads that must be built in to the structures.

Analysis of vapour cloud explosions which have actually occurred [1] has proved that blast effects are potentially devastating up to large distances from

* To whom correspondence should be addressed.

the centre of explosion. Significant blast effects are generated only if the energy is released in a short period of time, which means that the flame speed must be high.

One of the explosion regimes which could occur, is the detonation of the inflammable part of the unconfined cloud. Detonation is the most severe explosion regime, producing high velocity up to 1900 m/s and pressures up to 17 bars. But in view of the very large ignition energies required to directly initiate the detonation of a fuel–air mixture [2], near an optimum concentration, this detonation regime can be ruled out in practical conditions.

The other explosion regime is deflagration, which is more likely and which can also explain damage observed in all past accidents [3]. To judge the severity of such an explosion regime, an important research effort has been done to characterize the nature and the effects of deflagrations. A wide variety of tests, from small scale tests (at laboratory scale) to large scale (on open field) have been performed, so that there is now a considerable data base available on fuel–air deflagrations and pressure effects due to deflagrative explosions.

The present chapter is concerned with deflagration tests of unconfined inflammable fuel–air mixtures, without turbulence. We review field and laboratory experiments which may provide information on the deflagration of an unconfined vapour cloud. The objectives are as follows:

(a) a very short description of deflagration modellings used for analyzing and interpreting deflagration tests;

(b) a list of deflagration experiments whose data are presently available, including their conditions and configurations,

(c) a study and discussion of the main factors which may influence the combustion regime:

- effects of the concentration (homogeneous and heterogeneous media),
- effects of the cloud shape,
- effects of the energy released by ignition,
- effects of the size of the cloud.

2. Deflagrative explosion models: A brief survey

The simplest way to simulate an unconfined fuel–air mixture deflagrative explosion and to measure the blast generated, is to enclose into a slight confinement a uniform well-monitored composition of the inflammable mixture. Usually, the confinements are of spherical, hemispherical on the ground, pancake, cubic or rectangular shapes. The mixture boundary is formed by a soap film in laboratory scale experiments, and a rubber or plastic sheet in field experiments. When ignited at the center of symmetry, the mixture supports, in the absence of any obstacle or partial confinement, the propagation of a diverging spherical flame front. Furthermore, if pressure wave reflections, due to impedance mismatching on the interface at the sheet are ignored (an assumption which will be shown not strictly valid in the next items), the flame

expansion, free of any turbulence, occurs as in an infinite homogeneous medium. In such a situation, the flame history being known, the generated flow field can be calculated as described in the present item.

2.1 The spherical expanding flame model

All the above described conditions being fulfilled, the spherical expanding flame front may be thought as a thin discontinuity (compared to any characteristic observation length in the hydrodynamic field generated by the flame) which confines the burnt gases in a state of zero velocity. The spatial velocity (or speed) V_F of the front is therefore given by:

$$V_F = \beta S_u \tag{1}$$

where S_u is the apparent burning velocity which can be estimated from laminar burning velocity value S_u° (if the front instability is taken into account for correction) for most of hydrocarbon and hydrogen–air mixtures. The expansion ratio β is the density ratio of fresh to burnt gases calculated at the front discontinuity which supports a very small pressure drop for moderate flame velocities V_F. Consequently β is quite well estimated by the ratio of the adiabatic flame temperature (at ambient pressure) of the mixture to the ambient temperature (perfect gas assumption). If R_o is the radius of the initial unburnt mixture (initial radius of the spherical balloon), mass conservation implies that the final flame radius R_m (maximum radius of the flame ball) be given by:

$$R_m = \beta^{1/3} R_o \tag{2}$$

Experiments [4] with hydrocarbon–air mixtures of nearly stoichiometric composition – equivalence ratio ϕ roughly in the range 0.9 (lean) to 1.2 (rich) – show that a good estimate of β is around 8. This experimental value is smaller than the calculated adiabatic one [5]. Proofs of the existence of radiative losses from burnt gas to the surroundings were observed with large balloons [4] which could explain the β deficit. Notice, for $\beta \sim 6$, relation (2) gives

$$R_m \sim 1.8 R_o \tag{3}$$

To estimate the flame velocity from relation (1), care must be taken to select an appropriate value of the apparent burning velocity S_u. Numerous experiments (see, for instance Refs. [6, 7]) demonstrated that a cellular structure appears for most fuel–air mixtures (hydrocarbon, hydrogen) when the flame radius r_F reaches about 5 to 10 cm, and the actual flame front surface is augmented compared to the smooth spherical flame surface having the same mean radius. Large balloon experiments [8] and analytical treatment [9] are in agreement to estimate surface increase by a factor k of the order of 1.5 to 2.5. This factor must be included in relation (1) to get the actual value of V_F for large flame radius, multiplying the laminar value S_u° by the factor k. Even at very large flame radius r_F ($r_F > 5$ m in Ref. [8]), self-generated turbulence effects

do not appear. Only obstacles, like grids as in the experiments by Wagner et al. [10], are able to acceleratre sufficiently the flame front to give an apparent burning velocity to be included in relation (1), up to eight times the laminar value S_u^o.

2.2 Calculation of the hydrodynamic field

For moderate flame speed (compared to the sound velocity in burnt gases) the assumption of gas at rest in the flame ball is valid. Therefore, the flow field generated by the expanding spherical flame may be thought of as the field created by an equivalent spherical piston. For constant flame speed, this approach has been pioneered by Taylor [11], solved numerically by Kuhl et al. [12] as a limiting case of blast wave, and more recently, described analytically by Deshaies and co-workers [13–15].

For faster flames and detonative explosions, a number of numerical codes are now available (see, for instance, Refs. [16, 17]) for computation of blast pressure. As they are discussed in a separate chapter of this issue, only the model by Deshaies [7, 18] will be discussed here in more detail, because it is very appropriate to flow field calculations in the case of balloon experiments.

In this model [7] the flow is divided into three consecutive zones: (i) near the flame front an incompressible source flow; (ii) for distance $r > 2r_F$, r_F denoting the flame radius, the incompressible zone matches with an acoustic source flow; (iii) the acoustic zone is fitted to the leading zone entering the undisturbed medium at rest. The leading zone consists in an acoustic wave, unless the flame speed exceeds about 130 m/s. In this latter case, the leading pressure wave becomes a shock wave whose amplitude increases with the flame speed. Adopting this division of the flow into three zones, a complete field solution was found for a constant velocity flame of any speed [14]. The solution allows the pressure and velocity profiles versus time t at a given distance r (or versus distance r at a given time t) as shown on the schematic representation of Fig. 1, to be drawn as soon as the constant value of V_F is known.

The interesting fact, with respect to the interpretation of balloon experiments, is that the first order of the solution corresponding to constant velocity flames, can be extended to the case of variable flame velocity, provided that the flame accelerations remain moderate to prevent the formation of shock waves in the flow field. For clarity, the relationships giving the pressure and velocity fields generated by the expanding spherical flame whose path is given by the function $r_F(t)$, are reproduced here from Ref. [18]. The overpressure $\Delta p(r, t) = p(r, t) - p_o$ and velocity $u(r, t)$ in the environment of density ρ_o at pressure p_o, are given at the first order and at distance r respectively by:

$$\Delta p = \frac{\rho_o(1-\beta^{-1})}{r}\left(2r_F\left(\frac{dr_F}{dt}\right)^2 + r_F^2\left(\frac{d^2r_F}{dt^2}\right) - \frac{1-\beta^{-1}}{2}\frac{r_F^4}{r^3}\left(\frac{dr_F}{dt}\right)^2\right) \quad (4)$$

$$u = (1-\beta^{-1})\frac{r_F^2}{r^2}\left(\frac{dr_F}{dt}\right) \quad (5)$$

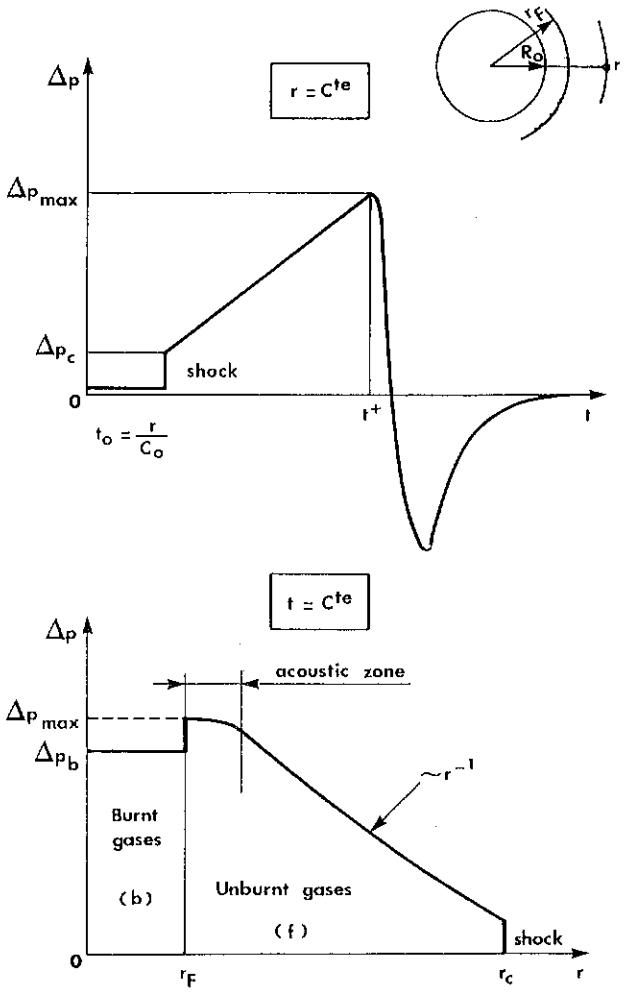

Fig. 1. Typical overpressure records by a spherical flame expanding at constant velocity: (a) versus time at a fixed distance r from the ignition point; (b) versus distance at a fixed time t. Notice that the shock wave indicated is an acoustic wave for flame speed V_F below 130 m/s.

near the front ($r \sim r_F$), and by

$$\Delta p = \frac{\rho_o(1-\beta^{-1})}{r}\left(2r_F(\tau)\left(\frac{dr_F(\tau)}{d\tau}\right)^2 + r_F^2\left(\frac{d^2r_F(\tau)}{d\tau^2}\right)\right) \tag{6}$$

$$u = (1-\beta^{-1})\left\{\frac{r_F^2(\tau)}{r^2}\left(\frac{dr_F(\tau)}{d\tau}\right) + \frac{1}{rc_o}\left[2r_F(\tau)\left(\frac{dr_F(\tau)}{d\tau}\right)^2 + r_F^2(\tau)\left(\frac{d^2r_F(\tau)}{d\tau^2}\right)\right]\right\} \tag{7}$$

in the acoustic zone ($r_F > 2R_0$). R_0 designs the initial radius of the inflammable volume and in relations (6) and (7), $\tau = t - r/c_0$, is the time variable, c_0 the sound velocity in the undisturbed medium.

Relationship (6) can be rewritten in the following form:

$$p(r, t) - p_0 = \frac{\rho_0(1-\beta^{-1})}{4\pi r} \frac{d^2 V}{d\tau^2} \tag{8}$$

which contains explicitly the acoustic source volume V whose variations versus time defines completely the monopole acoustic source strength, provided the expansion ratio β of the mixture may be considered as a constant.

The acoustic approach has been followed by several authors. Strehlow [19] used it to characterize the maximum peak overpressure generated by a pancake- or cigar-shaped cloud with central or edge ignition. A more sophisticated model, involving a distribution of simple sources successively activated according to the law of flame development, was proposed by Auton and Pickles [20] to exhibit the asymmetry of the pressure field in case of a cigar-shaped cloud ignited from the center. A similar model has been developed by Catlin [21] for non-spherical clouds lying on the ground with different aspect ratios. These latter calculations were found to agree fairly well with the results of experiments at small scale carried out with cylindrical clouds, point ignited on ground at the centre [22].

In the frame of acoustic models, it should be noticed that the pressure field depends not only on the flame speed V_F, but also on its variations (see relation (6)). Moreover the contribution of flame acceleration (or slowing down) to the pressure field is proportional to the squared flame radius. This important fact should not be ignored in practical situations of very large cloud: A final flame acceleration may lead to severe peak overpressures, although the flame speed be moderate during the main part of its travel across the cloud. One should say, however, that numerical blast calculations [17, 23] demonstrate that this effect is less and less pronounced as the mean flame speed is increased.

To conclude this brief review of the deflagrative explosion models, we will retain, for the next, the following statements:

1. The flow field generated by an unconfined constant velocity spherical flame is completely known.

2. A first order solution is available to describe the near field and the acoustic field taking into account the flame speed variations provided that the front mean velocity remains moderate (below about 130 m/s). The flame accelerations should be also sufficiently moderate to prevent shock-wave formation in the field.

3. Acoustic simple source models can be extended using an appropriate source array to take into account non-spherical shape and edge ignition. In that case, directional effects appear in the hydrodynamic field of the unconfined explosion.

3. The review of experiments on deflagrative unconfined explosion

A great need exists for data for the estimation of blast yields by accidental explosions and also for validation of the theoretical predictions. This is the main objective of laboratory and field experiments on unconfined deflagrative combustion without turbulence.

All the models just reviewed demonstrate that the pressure field depends not only on the flame speed but also on its time variations. Moreover, models show that the overpressure can be determined only in the case where the complete flame history is known in detail. These predictions can be accepted for practical use if there are reliable experimental results with which they can be compared.

The test programs conducted up to now cover generally four distinct topics whose objectives are as follows:

(1) *The concentration effect*: tests with homogeneous mixtures have been performed to study the influence of spontaneous acceleration of the deflagration and to validate models of the pressure field generated by a deflagration; Similarly, tests in non-uniform composition mixtures have been carried out to observe the flame acceleration effects produced by fuel concentration gradients which would occur in a real explosive cloud.

(2) *The shape effect*: to study the influence of the initial shape of the inflammable volume on the pressure field produced, a number of tests with various geometries (spherical, cylindrical, pancake and very complex shape of a real drifting cloud) have been run.

(3) *The size effect*: tests have been performed to characterize the effects of the explosion scale, when the volume of the inflammable charge is increased in a wide range from a volume of some liters up to several thousands of cubic meters.

(4) *The ignition effect*: the effect of energy released by ignition on the explosion regime obtained and on consequent flame speeds has been experimentally determined.

The influence of these four parameters is discussed in some detail in the following section. It is clear that all the experiments have a direct relevance to accidental explosions which have actually occurred as well as theoretical interest.

A complete list of the experiments, of which we are aware, on unconfined deflagration without turbulence is given in Table 1.

The expression "without turbulence" means that the flame trajectory is not affected by semi-confinements, by hot gases turbulent jet ignition, by crossing obstacles like grids, and the like, that is, in short, not affected by any cause liable for producing turbulences in the flow of unburnt gases and, as a result, forced accelerations of the flame.

TABLE 1

List of experimental conditions of the main balloon type experiments reported in the literature

No.	Tests	Year	Principal reference	Fuel	Volume	Geometry	Number of tests
1	Shell	1965	[27]	Ethylene Propane Methane Hydrogen	Small	Spherical (soap bubble)	A number
2	Nantes	1970	[28]	Natural gas	• Instantaneous 3 m^3 liquid • Continuous 0.17 m^3/min	Real cloud	40
3	China Lake	1975	[8]	Methane	262 m^3	Hemispherical	3
		1977		Propane Ethylene Ethylene oxide	2095 m^3		6 1 2
4	ENSMA	1979	[18]	Hydrogen Methane Propane Ethylene (+oxygen argon)	30 dm^3	Spherical or hemispherical (soap bubble)	A number
5	ENSMA	1980	[22]	Ethylene	17 dm^3	Cylindrical (soap bubble)	A number
6	Shell–Maplin Sand	1980	[29]	Natural gas	Spills • Continuous 2.8–5.8 m^3/mm	Real cloud	7 4
				Propane	• Instantaneous 5–12 m^3		
7	Charles 1	1981	[4]	Ethylene Acetylene	12 m^3	Spherical	12

Objective	Destruction of the enclosure	Topography	Concentration	Measures		Ignition
				Pressure	Flame trajectory	
Study of the noise produced by a flame		Laboratory	—	1 Acoustic microph.	High-speed camera	Electrical spark
Extent of a cloud	No confinement	Open field	A number	—	Photography	Torch
Flame propagation and flame acceleration process Unconfined or partially confined medium	No	Open field	—	10	High-speed camera	Weak source
Spontaneously accelerating flames	Yes	Laboratory	1 partial pressure	1	High-speed camera	Discharge of a capacitor or low energy spark
Effects of the deflagration of a pancake-shaped cloud	No confinement	Laboratory	1 partial pressure	1	High-speed camera	Low energy spark
Measurement of flame propagation and pressure waves generated by the deflagration of a real cloud (after a liquified gas spill on water)		Open field	200	24	Video	Spark ignition (number = 10)
Homogeneous medium–Influence of spontaneous acceleration on pressure	Yes and no	Open field	1	8	High-speed camera	Low energy electric ignition

TABLE 1. Continued

No.	Tests	Year	Principal reference	Fuel	Volume	Geometry	Number of tests
8	KWU	1981	[24]	Hydrogen	7.5 m^3 50 m^3 260 m^3 2100 m^3	Hemispherical	7 3 2 1
9	Coyote (3, 5, 6, 7)	1981	[30]	Natural gas	LNG spill 14.6 m^3 28.0 m^3 22.8 m^3 26.0 m^3	Real cloud	4
10	TNO	1982	[31]	Propane	Up to 1000 kg between flammability limits	Real cloud	10
11	Charles 2	1982 1983	[8]	Ethylene	12 m^3	Spherical	11
12	Charles 3	1983	[4]	Ethylene	12 m^3	Spherical	11
13	Shell	1983 1984	[32]	Natural gas Propane	3700 m^3	Cylindrical (segment of a pancake–shaped cloud)	15
14	Charles 4	1984	[4]	Ethylene	125 m^3	Half cubical (6.3 × 6.3 × 3.15)	3

Objective	Destruction of the enclosure	Topography	Concentration	Measures		Ignition
				Pressure	Flame trajectory	
Influence of cloud extension and ignition energy on flame speed	No	Open field	—	10	High-speed camera	Highly variable up to 1000 J (exploding wires)
Vapour burn experiments after liquified natural gas flame propogation	No confinement	Open field	89	2	Flame velocity sensors and photography	Flames or jet ignition
Effect of obstacles, but some unobstructed tests have been carried out (vaporization from a pond)	No confinement	Open field	—	A number	Video flame	Pyrotechnic ignition
Acceleration effects produced by fuel concentration gradients	Yes	Open field	2	8	High-speed camera	Low energy electric ignition
Effects of energy released by ignition	Yes	Open field	1	8	High-speed camera	Low energy electric ignition +plastic charge
Effects of obstacles and jet ignition: Unobstructed tests with natural gas Unobstructed tests with propane Unobstructed tests with jet ignition	Yes	Open field	7	9	Flame dectors and high-speed camera and video	Low energy or jet ignition
Effects of the size of the flammable cloud	Yes	Open field	3	8	High-speed camera	Low energy electric ignition

In Table 1, the principal features of the experimental campaigns are specified and in columns, one can find successively:

- the principal reference where the tests concerned are described extensively;
- the fuels used, which involve a large scale of reactivity, ranging from methane (the less reactive fuel) to very reactive fuels such as acetylene or hydrogen,
- the volume experimented;
- the configuration and geometry;
- the purpose of the tests and the phenomena studied;
- the surrounding topography;
- the extent of measurements: concentration, pressure, time of arrival of the flame, etc.;
- the type of ignition device.

Note that three different types of experiments are quoted in the table:

1. *Laboratory-scale experiments* which are very useful. Generally, the inflammable mixture is contained in a soap bubble and is ignited at its centre of symmetry or at the edge, the confinement by the bubble wall does not affect the flame development. Such small scale tests allow isolation of some process occurring in the deflagration and they can easily be multiplied.

2. *Enclosure-type experiments* (intermediate or large scale) which include balloon or pancake experiments. The simulated inflammable cloud is held in a thin bag, as shown on the typical arrangement of Fig. 2, and the mixture burns when ignited. In some tests, the balloon skin is destroyed before ignition,

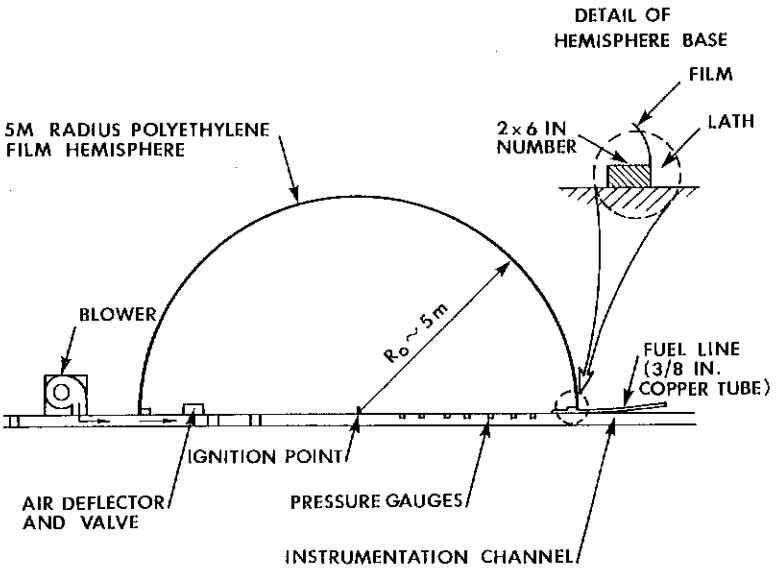

Fig. 2. Typical experimental arrangement for balloon-type experiments in medium-size scale (from Ref. [8]).

and the combustible mixture is in contact with the atmosphere as the flame front travels across the volume. In other tests, on the other hand, the destruction of the initial thin confinement is not operated. Particular attention is paid to this experimental procedure: indeed, a comparison between completely unconfined tests and other ones with a latex confinement of the charge (see, for instance, Ref. [4]) has shown that flame speeds are virtually the same during the first period of the propagation in the inflammable mixture and therefore the pressure field is unaffected; by contrast, the presence of a skin may have an effect on the final acceleration of the flame and the pressure signals may be different. Consequently, the overpressure values may be overestimated when the confinement is not removed before ignition (see also Section 4.1, below);

3. *Real cloud experiments* (at large scale) which allow the shape and the scale parameters to be investigated. Large quantities of inflammable materials are released, vaporized in the environment where an inflammable drifting cloud is formed, whose combustion is closely monitored. Flame speeds and overpressures are measured. The size of these tests is such that they represent a full-scale test for accident scenarios in an open space.

The influence on the unconfined deflagrative combustion of the principal parameters investigated is analyzed in more detail in the following paragraphs, on the basis of the experiments listed in the Table 1.

4. The main results

The flame speed and maximum overpressure ranges, observed in the different tests retained in the Table 1, are listed in Table 2. The analysis of this set of results allow the effects of fuel concentration (uniform or not), and of the cloud shape and size to be separated.

4.1 Effect of fuel concentration

4.1.1 The uniform composition mixtures

Results for uniform composition mixtures of common hydrocarbons and hydrogen with air are available (tests 1, 3, 7, 8, 14 in Table 2) in a large volume range: 10^{-5} to 4×10^3 m^3 approximately. The common feature to all these tests, is that the observed overpressures are always found between about 1 and 60 millibars, amplitudes which are unable to cause severe damage to the environment.

Generally speaking, the measured flame spatial velocity is well estimated by relation (1) in which the multiplying factor k is included to take into account the flame front folding. Three was found to be a rather conservative value for k. The expansion ratio β can be estimated from the maximum radius of the front and S_u^o taken as the classical laminar burning velocity of the fuel–air mixture for the given composition.

TABLE 2

Summary of results obtained from the experiments listed in Table 1

No.	Tests	Fuel	Concentration or equivalence ratio	Flame speed (m/s)	Overpressure (mbar) ($r \sim 2R_o$)	Comments
1	Shell (1965)	Hydrocarbons and Hydrogen	CH_4 C_2H_4 (9%) C_3H_8 H_2	3–20	0–0.6 (distance r ?)	Various compositions of superoxygenated air mixtures giving burning velocities as $0.4 < S_u^o < 1.9$ m/s
2	Nantes	Natural gas	Real cloud	5–15	Not measured	Real cloud
3	China Lake	Methane Propane Ethylene Ethylene oxide	10% 5% 6.5% 7.7%	5.2–8.9 6.1–12.6 17.3 13.4–22.5	— — — —	Balloon experiments
4	ENSMA (1979) (Spherical)	H_2 CH_4 C_3H_8 C_2H_4	Superoxygenated air, stoichiometry relative to O_2	3–100	1–350	Soap bubbles $2 < \phi < 40$ cm experiments with mixtures of volumetric composition as: $C_nH_m + YO_2 + ZN_2$ Y stoichiometry
5	ENSMA (1980) (cylindrical)	C_2H_4	Superoxygenated air, stoichiometry relative to O_2	3–50	1–150	$0 < Z < Z_{air}$
6	Shell–Maplin Sand	Natural gas Propane	Real cloud	< 10 < 28	< 0.8 < 0.4	
7	Charles 1	Ethylene Acetylene	1 1.3 1 1.8	8.5 11 11 17 20 32 17 38	3.3–5 6.4–21.6	Homogeneous

8	KWU	Hydrogen	Stoichiometry	<83.6	<60	Volume effect
9	Coyote	Natural gas	Real cloud	1–15 100	A few mbars	Real cloud Jet ignition
10	TNO	Propane	Real cloud	3–10 (in one test, 32 m/s)	0.3 (calculated)	
11	Charles 2	Ethylene	Concentration gradients	18–29	3.4–8.5	
12	Charles 3	Ethylene	1.1	<32	<12	
13	Shell	Natural gas Propane Natural gas	1.1 1.1 1.1	10 30 – 40 90–145	4–5 10–15 83–222	 Jet ignition
14	Charles 4	Ethylene	6.7%	11–20	12	

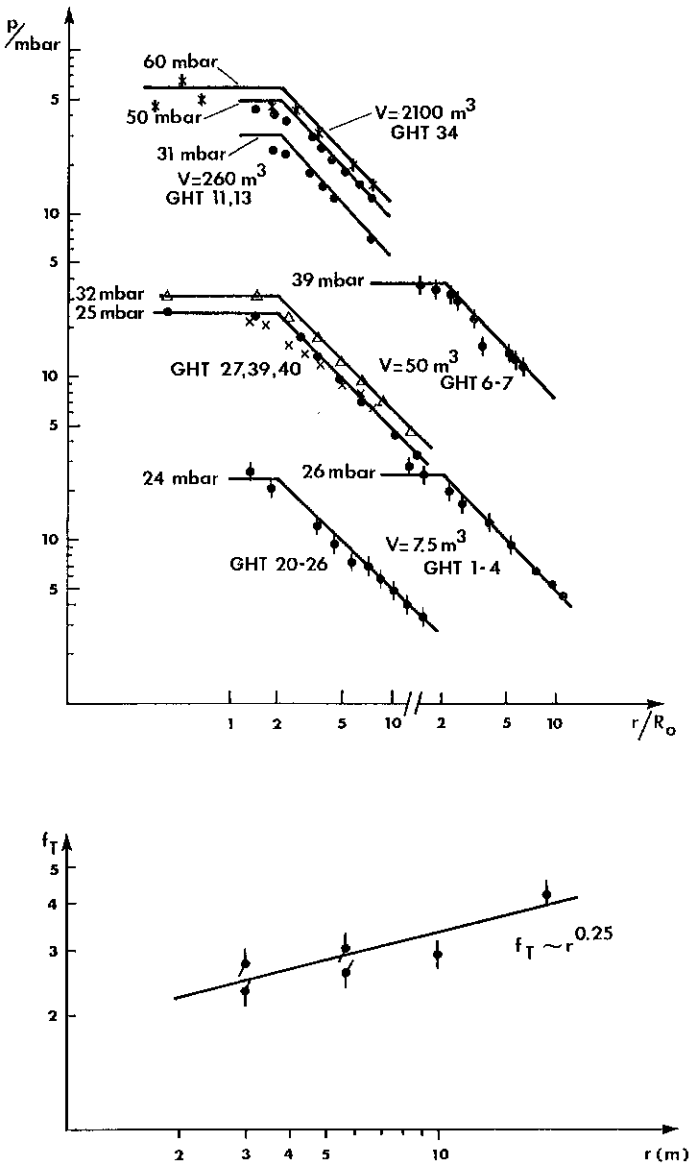

Fig. 3. Variations of overpressures versus distance (a), and flame velocity versus distance (b). Spherical explosion of H_2–air stoichiometric mixtures (from Ref. [24]).

The pressure field calculated from relations (4) to (7), or from analogous acoustic models, is in most cases in good agreement with the measurements. Figure 3 from Ref. [24] is an example of such an agreement for H_2–air mixtures at stoichiometry over a large volume interval: the peak overpressures exhibit

an acoustic behavior, decreasing outside the flame ball with the inverse of the distance r. Moreover, the constant pressure inside is related to the constant velocity spherical flame model (see Ref. [7] and Fig. 1) which can predict fairly correct values of the pressure signals.

Actually, even with uniform composition mixtures, the flame propagation velocity V_F is not a constant. Smooth successive spontaneous accelerations due to changes in the front structure are reported in Ref. [18] for small flames. Woolfolk and Ablow [25] noticed that the radius r_F of the fast spherical deflagration in H_2–O_2 stoichiometric mixtures (R_o=0.455 and 0.8 m) varies with time as:

$$r_F \sim t^{1.36} \tag{9}$$

that means a flame speed V_F increasing with time t as $t^{0.36}$. A similar behavior is reported in Ref. [24] for H_2–air mixtures for which the ratio of the actual flame speed to its laminar value increases with flame radius as $r^{0.25}$ (Fig. 3(b)). The flame front accelerates during the end of the propagating phase, several causes being involved in this behavior: (a) the balloon sheet is often maintained by a supporting device, acting as an obstacle (grids or so); (b) when the wall is destroyed before ignition — as in Charles 1 test — a perturbed, rippled interface is left between the mixture and the ambient air leading to a flame acceleration. This phenomenon is even observed (but slightly) with the light confinement offered by the soap film in bubbles experiments [5].

Pressure wave shape and amplitudes (see Fig. 1) and flame speed variations have been correlated in the acoustic region for some tests: starting from the recorded pressure signal versus time at a given distance r, the flame speed and flame path are reconstructed by two successive integrations of relation (6). This method, used in the Charles 1 test set [4] and in other tests has confirmed that the flame speed V_F was effectively increased (as clearly seen on the example of Fig. 4) at the moment when the flame radius became larger than approximately 1.5 m (the initial radius of the charge was R_o=1.4 m).

The consequence of the occurrence of an accelerated end phase is to yield peak overpressures higher (multiplied by a factor of 2 in some cases) than the peak pressure which would be observed at a constant flame speed (from ignition time to end of combustion) evaluated on the theoretical basis of relation (1).

4.1.2 Mixtures exhibiting a fuel concentration discontinuity

With the objective of assessing the influence of more severe accelerations of the flame, some experiments were performed at a laboratory scale [18] or at a medium scale (in Charles 2 tests [4] involving 12 m^3 of several ethylene–air mixtures), where a fuel concentration discontinuity was displayed along the flame path. Rich or poor compositions were associated to nearly stoichiometric ones to provoke noticeable variations in the flame speed. In the example of Fig. 5, the mixtures, initially confined within two concentric latex balloons of radii R_i=0.9 and R_e=1.4 m respectively, are ignited at the centre, and the flame propagates from rich (13% C_2H_4) to stoichiometric (8.5% C_2H_4)

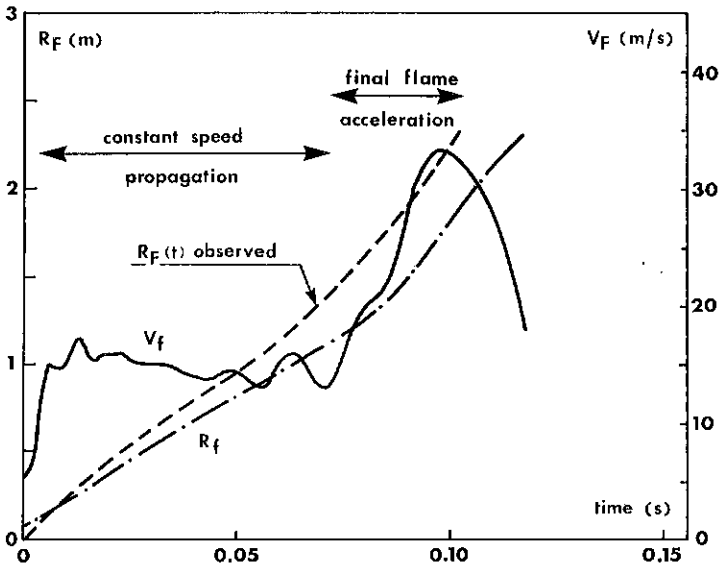

Fig. 4. Flame trajectory $r_F(t)$ and flame velocity $V_F(t)$ versus time in the case of a 12 m^3 deflagrative explosion of acetylene–air mixture (Charles 1 tests, Ref. [4]). Notice the flame acceleration in the final period of the propagation.

compositions. Instead of the expected flame acceleration at radius $r_F \sim 2R_i$, an oscillatory propagation was observed in the rich mixture ($0 < t < 90$ ms), followed by a constant speed travel at the transition between the two mixtures ($t \sim 100$ ms) and, curiously, the flame slowed down abruptly when burning the stoichiometric composition. Such behavior could probably be explained by the destruction of the balloon skins before ignition, allowing turbulences to be induced, and interdiffusion between the two mixtures and between the external mixture and air, to occur. Actually, in some Charles 2 tests where the balloons were not destroyed, normal behavior was observed: acceleration (or slowing down owing to fuel percentage) of the flame occurred at the interface of the inner balloon, and the peak pressure (enhanced by the confinement) corresponded to the end of burning of the fastest composition.

Generally speaking, the balloons were either destroyed or not before ignition and whatever the adjoining compositions, the maximum flame speeds were found to be larger by a factor of about 1.5 compared to the value observed with the fastest uniform composition (8.5% C_2H_4) experimented in Charles 1 tests. Consequently, the overpressure peaks found in Charles 1 tests, were multiplied by a factor of 2 to 3 by the influence of the composition discontinuity. Moreover, the pressure signals displayed severe oscillations, which could reinforce damages in real accidents as far as resonant effects on the structure are concerned in actual hazards.

Finally, the acoustic correlation (relation (7)) gave satisfactory results in the interpretation of the experiments as for the uniform compositions.

This behavior is illustrated in Fig. 6 where typical pressure signals from the deflagration of a hemisphere and of a cylinder of the same volume (C_2H_4–air stoichiometric) are compared. The flame speed, $V_F = 6$ m/s during the spherical phase, decreases to $V_F = 3.5$ m/s, for the cylindrical propagation which generates a nearly constant overpressure (the final peak due to the particular experimental arrangment of Ref. [22] should be ignored when there are no obstacles).

Typically, peak overpressure generated by the deflagration of flat volumes are significantly smaller than in the spherical case, and become very weak when the aspect ratio ε is reduced. This general conclusion is confirmed by larger scale experiments as shown on Fig. 7 and also by real cloud experiments

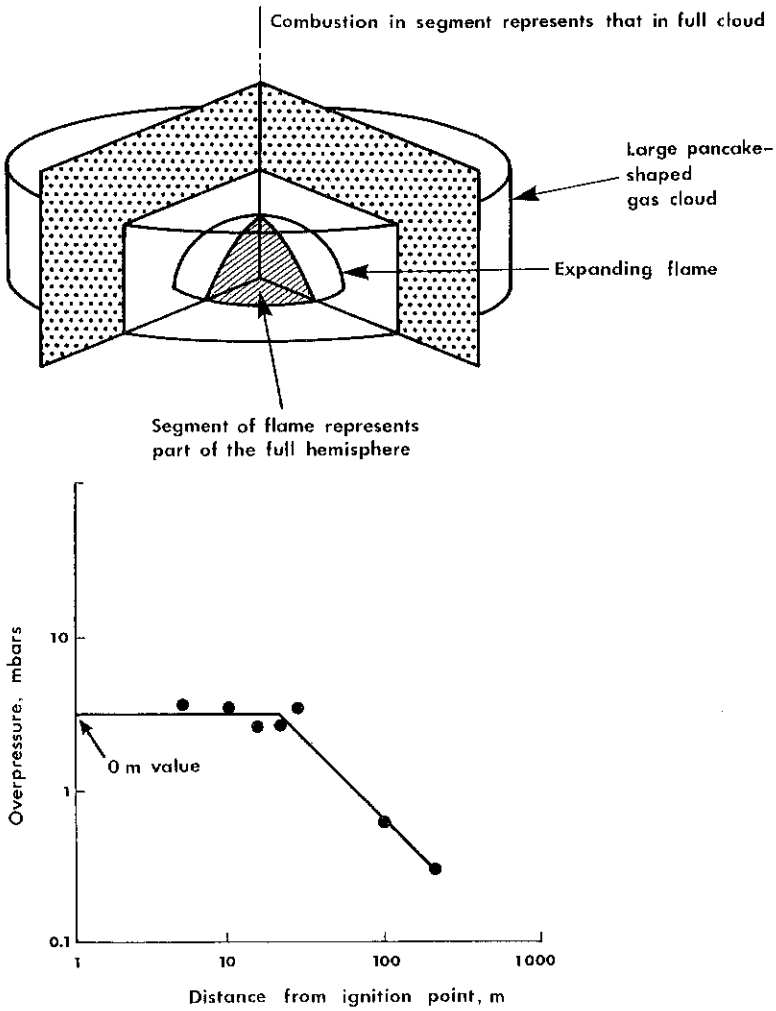

Fig. 7. Peak overpressure registered in large scale cylindrical unconfined explosions (from Ref. [32]).

such as 9, 6, 13 in Table 2. Even with fast flames ($V_F \sim 100$ m/s) observed with turbulent jet ignition, overpressures remain always in the range of a few millibars. Acoustic models (Refs. [18–22]) are very useful to explain the far field pressure, at least qualitatively. Near the exploding cloud, the pressure field may exhibit asymmetry [21] and non-acoustic decay of the wave.

4.3 Influence of the volume of the explosive mixture

As already mentioned in the above items, hemispherical balloons have been used to experiment up to about 2100 m^3. With central weak ignition and in the case of uniform mixture composition, there is a tendency for the spherical flame to accelerate continuously with increasing radius (see Refs. [24, 25] and Fig. 3). But the acceleration remains moderate, as evidenced by the results of Lind [8] given in Fig. 8 relative to propane and methane–air mixtures. So, one may expect more pronounced blast effects with large sized flames, but without any obstacles or turbulence the velocities are much lower than observed during a predetonation period or in confinements. The overpressures observed are far below 100 mbars, and then are non-catastrophic for the environment.

It should be noticed that buoyancy effects are observed for a spherical flame whose radius exceeds about one meter for hydrocarbon–air mixtures. As a consequence, the flame speed in the vertical direction is larger than in the horizontal one (see Fig. 8). This effect was also observed in Charles experiments with 125 m^3 of ethylene–air (6.7% C_2H_4) contained in a retractable rectangular box [4]. In this case, the measured pressure field was comparable to the calculated field taking into account the flame speed observed in the 45° direction. So buoyancy effects are certainly responsible for the asymmetry in the generated field but are of negligible influence on the overpressure values.

The negligible influence of the size of the mixture volumes on unconfined deflagrative explosion yields is further confirmed by large scale trials simulating real clouds. For instance, in tests 6, 9, 10 on Table 2, measured overpressure did not exceed a few millibars and flame velocities were lower than 15 m/s, as shown in Fig. 9.

4.4 Strong ignition energy

For the most part of the experiments performed, ignition energy was low (spark or fuse composition). If one expects ignition by hot jets, which involves turbulent propagation and for that reason is discussed elsewhere, strong ignition was studied in Charles 3 (see Table 2) only. Twelve cubic meters of ethylene–air mixtures (8.5%) were fired using the detonation of 5–8 g of a solid explosive and a deflagration was observed to propagate behind a decaying spherical shock wave. In the initial phase, the flame boosted by the shock was accelerated up to about 100 m/s, but the flame speed suddenly decreases around $r_F \sim 1$ m, and, completely decoupled from the shock wave, recovered an almost constant velocity of the order of 30 m/s (compared to about 12 m/s for weak ignition of the same mixture). As a consequence, in the far field, the leading shock wave generated by the solid explosive detonation having completely

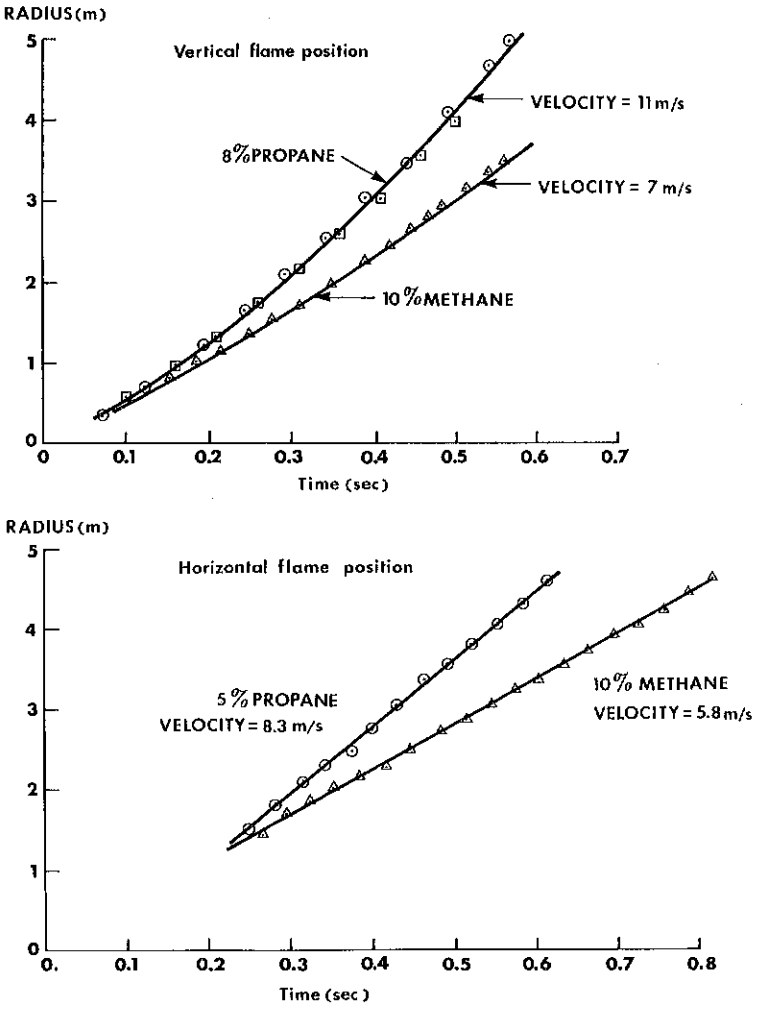

Fig. 8. Large scale balloon experiments. Illustration of buoyancy effects on the flame propagation (from Ref. [8]).

decayed, the peak overpressure observed was at most 10 mbars, as shown on Fig. 10, and thus was relevant for acoustic interpretation. It should be noticed that previous tests [26] demonstrated that 10–12 g of the same explosive were able to initiate the detonation of the ethylene–air mixture; but intermediate regimes of fast deflagration could never be generated even with accurate weighting of the explosive mass between 8 and 10 grams.

So it could be concluded that, even with sensitive mixtures, strong ignition without turbulence lead either to detonation or to slow deflagration. In the last case, fast deflagration at a speed of several hundred meters per second is restricted to the very beginning of the propagation which is not self-sustained.

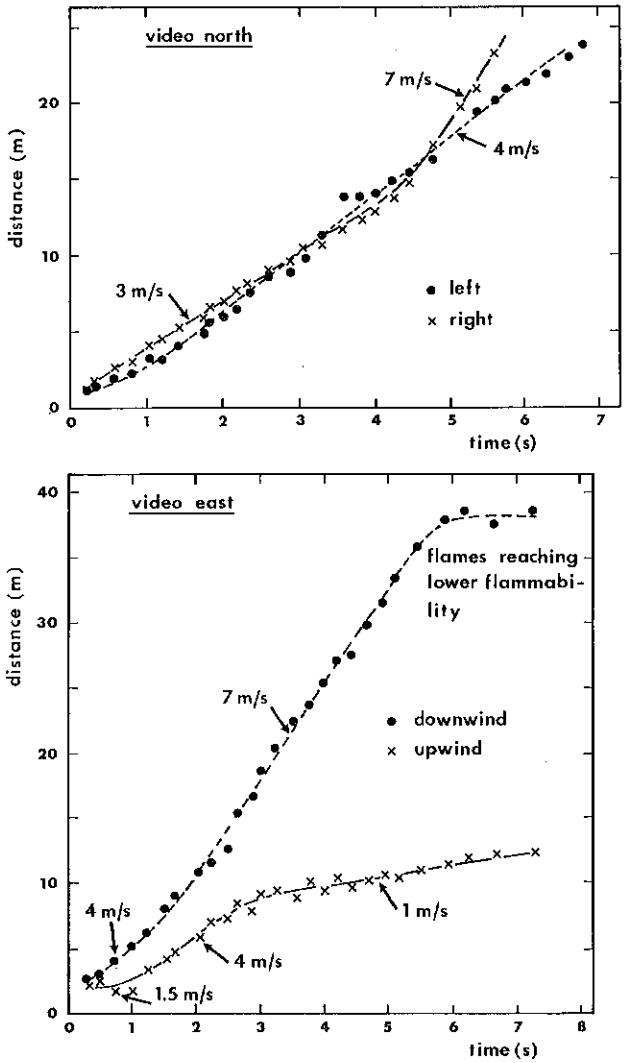

Fig. 9. Flame trajectories in real cloud explosion (from Ref. [31]). Propane–air cloud without obstacles.

5. Conclusion

The present chapter reviews several sets of experiments, at small, intermediate and large scale, which have been performed because of the lack of knowledge to predict the yields of unconfined deflagrative combustion.

The results of all these tests, without any source of turbulence generation, confirm the low values of the flame speed even for the more reactive fuels.

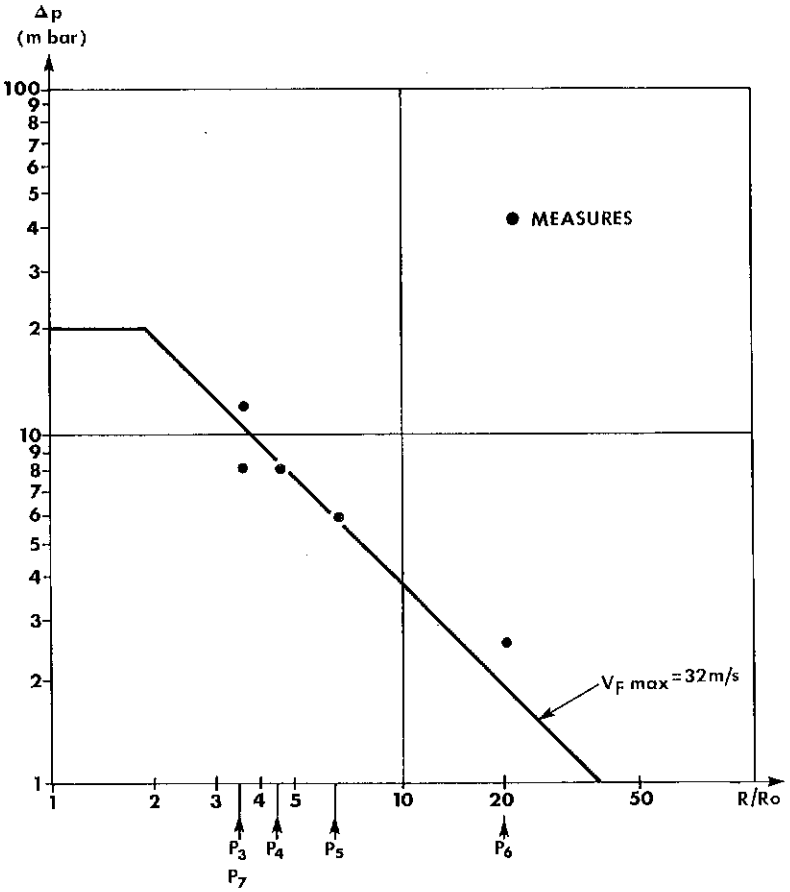

Fig. 10. Maximum peak overpressures versus distance observed with ethylene–air mixture in the case of strong ignition energy (Charles 3 tests Ref. [4]).

Experimental values of flame speed are of the order of 15 m/s, for an equivalence ratio of 1, except for hydrogen and acetylene which have had values of 30 m/s reported. As a result, truly unconfined fuel–air explosions produces very weak pressure effects, of the order of few millibars near the edge of the inflammable charge. No important scale effects have been observed.

The pressure field has been found to be highly dependent on the acceleration of the flame which could be generated either by the experimental device itself (especially at the boundary of the charge) or by fuel concentration gradients in the inflammable mixture. But they never cause an important increase in the peak overpressure to be observed, even if the cloud is ignited by a strong ignition source such as a solid explosive mass. However, ignition by hot turbulent jet issuing from a confinement should be treated with care.

In the light of pressure levels recorded in a completely open space, such conditions of explosion do not appear to be a major risk. The only causes of greater overpressures, capable of inflicting severe damage on structures, would be high energy ignition combined with semi-confinement effects, obstacles effects and hot jet ignition, able to create turbulences on the flame path. These effects are discussed in some detail in separate chapters of this issue.

Considering as well established by now, the fact that truly unconfined deflagrative explosions are not very powerful and are easily supported by the conventional structures of most of the industrial plants, one may doubt the interest in future balloon experiments. Obviously, they should be restricted to cases where primary information is needed on the reactivity of new fuels, or on mixtures of several conventional fuels. Indeed, balloon experiments without turbulences are easy to perform rapidly and at relatively low cost. However, in no case can such types of experiments simulate actual large scale deflagrative explosion hazards in which obstacles and partial confinements are of drastic influence.

References

1 W.E. Baker, P.S. Cox, P.S. Westine, J.J. Kulesz and R.A. Strehlow, Explosion Hazards and Evaluation, Fundamental Studies in Engineering 5, Elsevier, Amsterdam, 1983.
2 D.C. Bull, J.E. Elsworth and P.J. Shuff, Detonation cell structures in fuel/air mixtures, Combust. Flame, 45 (1982) 7.
3 A. Lannoy, Analyse des explosions air–hydrocarbure en milieu libre – Etudes déterministe et probabiliste du scénario d'accident – Prévision des effets de surpression, Bulletin de la Direction des Etudes et Recherches d'Electricité de France, Série A, no. 4, 1984.
4 J. Brossard, D. Desbordes, N. Di Fabio, J.L. Garnier, A. Lannoy, J.C. Leyer, J. Perrot and J.P. Saint-Cloud, Caractérisation du champ de pression induit par l'explosion aérienne d'un mélange air–hydrocarbure, déflagration lente, déflagration rapide, Rapport EUR 9679 FR, Commission des Communautés européennes, Brussels, 1985. See also, from the same authors, Truly unconfined deflagrations of ethylene–air mixtures, in M. Summerfield (Ed.), Progress in Astronautics and Aeronautics, Vol. 106, Am. Inst. Aeronaut. Astronaut., Washington, DC, 1986, pp. 90–106.
5 J.C. Leyer, C. Guerraud and N. Manson, Flame propagation in small spheres of unconfined or slightly confined inflammable mixtures. 15th Int Symp. on Comb., The Combustion Institute Publ., Pittsburgh, PA, 1975, pp. 645–653.
6 A.G. Istratov and V.B. Librovich, On the stability of gas dynamic discontinuities associated with chemical reactions: the case of a spherical flame, Acta Astronautica, 14 (1969) 453–467.
7 B. Deshaies, Les flammes sphériques: Propagation divergente et combustion stationnaire, Thèse de Doctorat ès Sciences, no. 329, University of Poitiers, Poitiers, France, 1981.
8 C.D. Lind, Explosion hazards associated with spills of large quantities of hazardous materials, Phase 1, Final Report No. CG-D-30-75, Department of Transportation, U.S. Coast Guard, 1974.
9 G.I. Sivashinsky, Non-linear analysis of hydrodynamic instabilities in laminar flames, Parts I and II, Acta Astronautica, 4 (1977) 1177–1206 and 1207–1221.
10 K.J. Dörge, D. Pangritz and H.G. Wagner, Experiments on velocity augmentation of spherical flames by grids, Acta Astronautica, 3 (1976) 1067–1076.
11 G.I. Taylor, Proc. R. Soc. A 186 (1946) 273–292.

12 A.L. Kuhl, M.M. Kamel and A.K. Oppenheim, On flame generated self similar blast waves, 14th Symp. Int. on Comb., The Combustion Institute Publ., Pittsburgh, PA, 1973, pp. 1201–1214.
13 B. Deshaies and P. Clavin, Effets dynamiques engendrés par une flamme sphérique à vitesse constante, J. Mécanique, 18(2) (1979) 213–223.
14 P. Cambray and B. Deshaies, Ecoulement engendré par un piston sphérique: solution analytique approchée, Acta Astronautica, 5 (1978) 611–617.
15 P. Cambray, B. Deshaies and P. Clavin, Solution des équations d'Euler associée à l'explosion d'une sphère à vitesse constante, J. Phys., Colloq. C8, 40 (1979) 11.
16 A.K. Oppenheim, J. Kurylo, L.M. Cohen and M.M. Kamel, Shock Tube Symp., 1979.
17 C.J.M. van Wingerden, A.C. van Den Berg and J.P. Zeeuwen, Validation of numerical codes for the simulation of blast generated by vapor cloud explosions, In: M. Summerfield (Ed.), Prog. Astronaut. Aeronaut., 106 (1986) 422–435.
18 B. Deshaies and J.C. Leyer, Flow field induced by unconfined spherical accelerating flames, Combustion Flame, 40 (1981) 141–153.
19 R.A. Strehlow, The blast wave from deflagrative explosions: an acoustic approach, In: 13th Loss Prevention Symp. AIChE, Philadelphia, PA, 1980. (Abstract book).
20 T.R. Auton and J.H. Pickles, The calculation of blast waves from the explosions of pancake shaped vapour clouds, Central Electricity Research Laboratories RD/L/N210/78, 1978, p. 17.
21 C.A. Catlin, An acoustic model for predicting the overpressure caused by the deflagration of a ground lying vapour cloud, British Gas R&D Report, MRS E443, 1985.
22 J.C. Leyer, An experimental study of the pressure fields by exploding cylindrical clouds, Combustion Flame, 48 (1982) 251–263.
23 A.C. Van Den Berg, Computational investigation of blast due to spherical non steady deflagrative flames using low flame speed explosion simulation model, Report No. PML 1982–107, Prins Maurits Laboratorium, Rijswijk, The Netherlands, 1982.
24 W. Drenckhahn and C. Koch, Transition from slow deflagration to detonation, Seminar on the Results of the European Committees Indirect Action Research Program on Safety of Thermal Water Reactors. CEC Meeting, Brussels, 1985, In: Safety of Thermal Water Reactors, Graham and Trotman, London, 1985, pp. 223–240.
25 R.W. Woolfolk and C.M. Ablow, Blast waves from non ideal explosions, Proc. of Conf. Mechanisms of Explosion and Blast Waves, Feltman Research Laboratory, Picatinny Arsenal, Dover, 1973, p. 42.
26 J. Brossard, J.C. Leyer, D. Desbordes, J.P. Saint-Cloud, S. Hendricks, J.L. Garnier, A. Lannoy and J. Perrot, Air blast from unconfined gaseous detonations, in: M. Summerfield (Ed.), Progress in Astronautics and Aeronautics, Vol. 94, 1984, pp. 556–566.
27. A. Thomas and G.T. Williams, Flame noise: sound emission from spark ignited bubbles of combustion gas, Proc. R. Soc. A 294 (1966) 449–446.
28 R. Humbert-Basset and A. Montet, Dispersion dans l'atmosphère d'un nuage gazeux formé par épandage de GNL sur le sol, GNL3 Congress, Washington, 1972. (Abstract book).
29 W.J.S. Hirst and J.A. Eyre, Maplin Sands Experiments 1980: Combustion of large LNG and refrigerated liquid propane yields on the sea, Second Symposium on Heavy Gases and Risk Assessment, Frankfurt-am-Main, Germany, 25–26 May, 1982. In: S. Hartwig (Ed.), Batelle Inst./D. Reidel, Colombus, OH/Dordrecht, 1983.
30 H.C. Rodean, W.J. Hogan, P.A. Urtiew, H.C. Goldwire, T.G. McRae and D.L. Morgan, Vapor burn analysis for the Coyote Series LNG Spill Experiments, Lawrence Livermore National Laboratory, Report UCRL 53530, Berkeley, CA, April 1984.
31 R.M. Dauwe, C.J.M. Wingerden and J.P. Zeeuwen, Experimental investigation into the blast effect produced by unconfined vapour cloud explosion, In: 4th Int. Symp. on Loss Prevention and Safety Promotion in the Process Industries, Harrogate, 12–16 September, 1983. AIChE event 290 of EFCE, Pergamon Press, London, 1983, pp. D20–D29.

32 A.J. Harrison and J.A. Eyre, The effect of obstacles and jet ignition on the combustion of gas clouds, In: 5th Int. Symp. on Loss Prevention and Safety Promotion in the Process Industries, Cannes, September 1986. Société de Chimie Industrièlle, Paris, 1967, pp. 38.1–38.13.